Vibrationally resolved structure in O_2^+ dissociation induced by intense ultrashort laser pulses

M. Zohrabi, J. McKenna, B. Gaire, Nora G. Johnson, K. D. Carnes, S. De, I. A. Bocharova, M. Magrakvelidze, D. Ray, I. V. Litvinyuk,* C. L. Cocke, and I. Ben-Itzhak

J. R. Macdonald Laboratory, Physics Department, Kansas State University, Manhattan, Kansas 66506, USA

(Received 21 February 2011; published 5 May 2011)

Laser-induced dissociation of O_2^+ is studied in the strong-field limit using two independent methods, namely a crossed laser–ion-beam coincidence 3D momentum imaging method and a supersonic gas jet velocity map imaging technique (790 and 395 nm, 8–40 fs, $\sim 10^{15}$ W/cm^2). The measured kinetic energy release spectra from dissociation of O_2^+ and dissociative ionization of O_2 reveal vibrational structure which persists over a wide range of laser intensities. The vibrational structure is similar for O_2^+ produced incoherently in an ion source and coherently by laser pulses. By evaluation of the potential energy curves, we assign the spectral energy peaks to dissociation of the $v = 10$–15 vibrational states of the metastable $a\,^4\Pi_u$ state via the dissociation pathway $|a\,^4\Pi_u\rangle \rightarrow |f\,^4\Pi_g - 1\omega\rangle$—a mechanism equivalent to bond softening in H_2^+.

DOI: 10.1103/PhysRevA.83.053405 PACS number(s): 33.80.Wz, 42.50.Hz

I. INTRODUCTION

Intense ultrashort laser pulses have many applications in the physical, chemical, and biological sciences as they provide an opportunity to manipulate reaction dynamics. In particular, they have proven invaluable for imaging and controlling molecular dynamics through their nonlinear interaction with molecules (e.g., Refs. [1,2]). Typically, however, molecular imaging in strong laser fields has been limited to electronic states (e.g., Refs. [3–8]), as high-resolution studies of individual vibrational (v) states in strong fields are challenging and rare. The ability to perform v-state-specific studies, for example, opens the door to better control of molecular reactions as each v state can react in a different way to the strong laser field [9]. With advances in time- and position-sensitive imaging detectors, and better imaging techniques such as reaction microscopes [10,11] and velocity map imaging (VMI) [12,13], experimentalists are in a better position to target v-state-selective studies.

One place to look for vibrational structure, which survives the strong-field interaction with a molecule, is in the dissociative ionization of H_2. This process involves dissociation dynamics of the intermediate one electron H_2^+ molecule. Generally, only two electronic states are involved in H_2^+ dissociation dynamics, the $1s\sigma_g$ ground state and the $2p\sigma_u$ first excited state. Higher-lying electronic states can be neglected in most cases, although they do occasionally play a role (see, e.g., Refs. [14–16]). In spite of the simplicity of, and the multitude of studies on, H_2 [17,18], observations of vibrational structure in its dissociative ionization, such as that by Zariyev *et al.* [19], are extremely rare. Indeed, this study was carried out using relatively long laser pulses (160 fs) that have a narrow bandwidth, which is good for spectral resolution but not amenable to time-resolved imaging experiments.

In contrast, vibrational resolution studies of H_2^+ ion beam targets are considerably more common [20–26]. Typically the high v states of H_2^+ dissociate by one-photon excitation to the repulsive $2p\sigma_u$ state on the low-intensity leading edge of the laser pulse, a fact that helps preserve the vibrational energy structure upon dissociation.

It is less intuitive that vibrationally resolved structure will appear in dissociation of more complex diatomic molecules driven by strong fields [27]. Normally the large multitude of potential energy curves and possible dissociation pathways, even in relatively simple systems like N_2^+ or O_2^+, can lead to interference between pathways, or overlap in kinetic energy release (KER) peaks, that simply inhibit the observation of vibrational structure. Arguably this is the main reason for the absence of vibrationally resolved spectra in such molecules to date.

In light of these issues, it is perhaps surprising that we do observe vibrational structure in strong-field dissociation of a multielectron molecule, O_2^+—as we present here. Using intense 790-nm, 395-nm, 40-fs pulses, we demonstrate clearly the presence of structured peaks in the KER spectrum following dissociation of an O_2^+ ion beam target that can be assigned to specific v states. Even more surprising, we have observed the equivalent structure in the dissociative ionization of an O_2 gas target with even shorter pulses of 8 fs (FWHM). It is important to note that these two targets differ in how O_2^+ is prepared—a *coherent* vibrational wave packet if starting from an O_2 gas target and an *incoherent* ensemble of v states if starting from an O_2^+ ion beam target [22,28,29].

Our choice of O_2^+ to look for vibrational structure is triggered by the fact that we have explored this system previously with an intense laser, particularly its dissociation as an ion beam [30,31]. From this earlier work we believe that we can identify a large number of its dissociation pathways. Unfortunately, at that time our imaging resolution for the ion beam fragments was insufficient to discern vibrational peaks in KER had they been present. After significant development of our crossed-beam coincidence 3D momentum imaging setup we can now measure vibrationally resolved KER spectra in H_2^+ [24], and also in low energy dissociation of O_2^+, presented in this work.

II. EXPERIMENTAL METHOD

The laser used for these studies is a Ti:sapphire chirped-pulse amplification system operating at a repetition rate

*Present address: Centre for Quantum Dynamics, Griffith University, Brisbane, Queensland 4111, Australia.

of 1.5 kHz, with an output central wavelength of 790 nm, a Fourier-transform-limited pulse duration of 40 fs (FWHM in intensity), and a pulse energy of up to 1 mJ. The pulses can be compressed in duration to 8 fs using a hollow-core fiber filled with neon gas and a chirped mirror compressor or, alternatively, converted in wavelength to 395 nm using a second-harmonic-generation β-barium borate crystal. The linearly polarized pulses are either focused onto the O_2^+ ion beam target using an $f = 203$ mm off-axis parabolic mirror, generating intensities up to 4×10^{15} W/cm^2, or back-focused onto the O_2 supersonic gas-jet target by an on-axis $f = 75$ mm spherical mirror, generating the 10^{14} W/cm^2 intensity used in our VMI measurement.

For our O_2^+ ion beam measurements, oxygen gas was ionized by electron impact in an electron cyclotron resonance (ECR) ion source. This produced O_2^+ ions with about one-third of the molecules in the metastable lowest quartet state, $a\,^4\Pi_u$, and the remaining two-thirds in the doublet ground state, $X\,^2\Pi_g$ (see, for example, Ref. [32,33]). The approximately Franck-Condon vibrational populations of these two electronic states differ, as shown in Figs. 1(a) and 1(b). As will be shown later, the main channel of interest in this study involves the dissociation of the $a\,^4\Pi_u$ state.

Following acceleration and momentum selection of the ions, the 7-keV O_2^+ beam was transported to the laser interaction region where it was crossed orthogonally by the focused laser beam, with the laser polarization oriented perpendicular to both beam directions. The choice of ion beam energy was a compromise, maintained low to improve the KER spectral resolution but high enough to assure an acceptable detection efficiency, especially for the neutral fragments. A static electric field applied in the interaction region using a longitudinal spectrometer accelerated the charged molecular fragments toward a time- and position-sensitive detector such that all fragments, neutral and ions, were separated by time-of-flight (TOF) and measured in coincidence. The primary O_2^+ beam was collected in a small on-axis Faraday cup. Therefore, this measurement relied on the fragments having sufficient dissociation momenta transverse to the O_2^+ beam to separate them from the Faraday cup—with the drawback that those that had insufficient energy (KER $\lesssim 0.1$ eV) were blocked.

Our coincidence imaging technique allows us to cleanly separate the dissociation channel of interest, namely O^++O, from other dissociative ionization channels. For this channel, we evaluate the momenta of both dissociating fragments from the TOF and position information, recorded event by event, therefore retrieving the complete kinematic information about the process under study. From these momenta the KER and the direction of the dissociating fragments (θ,ϕ) relative to the laser polarization are determined (see further details in our previous publications [22,28–31]).

III. RESULTS AND DISCUSSION

A. O_2^+ beam target

Typical dissociation spectra for O_2^+ are shown in Fig. 2. The angle θ is between the molecular dissociation axis and the laser polarization. This spectrum is rich in structure and many of the dissociation pathways responsible for the features have been identified in our earlier work [30], as well as by others (e.g., Ref. [36]). Specifically, the peak labeled α at about 2.3 eV is due to three-photon absorption via the pathway $|a\,^4\Pi_u\rangle \rightarrow |f\,^4\Pi_g - 3\omega\rangle$ [30]. The peak labeled β at about 1.5 eV can be assigned to the more complex dissociation pathway $|a\,^4\Pi_u\rangle \rightarrow |f\,^4\Pi_g - 1\omega\rangle \rightarrow |^4\Sigma_u^+ - 2\omega\rangle$. Additionally, the peak labeled γ at about 0.7 eV is associated with dissociation

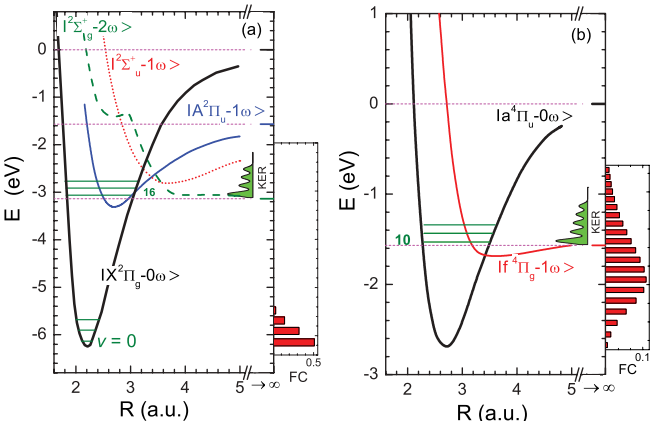

FIG. 1. (Color online) Diabatic dressed potential energy curve (PEC) diagram of O_2^+ depicting the main dissociation pathways (see text) of the (a) $X\,^2\Pi_g$ doublet ground state and (b) $a\,^4\Pi_u$ lowest quartet state, yielding low KER. The PECs were taken from Ref. [34]. The vibrational populations, shown in the insets, are the Franck-Condon (FC) factors for vertical electron-impact ionization in the ion source. We used the phase-amplitude method [35] to evaluate the vibrational wave functions needed for the overlap integrals. A schematic vibrationally resolved low-KER spectrum is also shown in each panel.

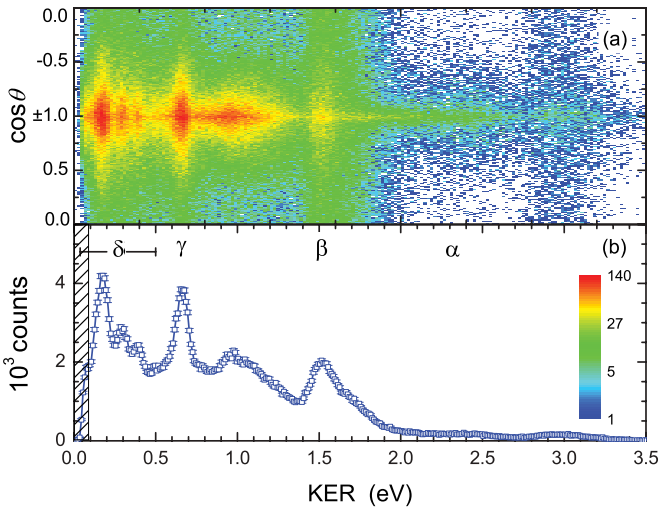

FIG. 2. (Color online) (a) KER-cosθ density plot of O_2^+ dissociation in a 790 nm, 40 fs, 4×10^{15} W/cm^2 laser pulse. (b) the KER spectrum evaluated by integrating over all angles in panel (a). The labeled KER peaks are associated with the following dissociation pathways (see text): (α) $|a\,^4\Pi_u\rangle \rightarrow |f\,^4\Pi_g - 3\omega\rangle$, (β) $|a\,^4\Pi_u\rangle \rightarrow |f\,^4\Pi_g - 1\omega\rangle \rightarrow |^4\Sigma_u^+ - 2\omega\rangle$, (γ) see Ref. [37], and the feature of main interest here (δ) $|a\,^4\Pi_u\rangle \rightarrow |f\,^4\Pi_g - 1\omega\rangle$ for $v = 10$–15 – depicted in Fig. 1(b).

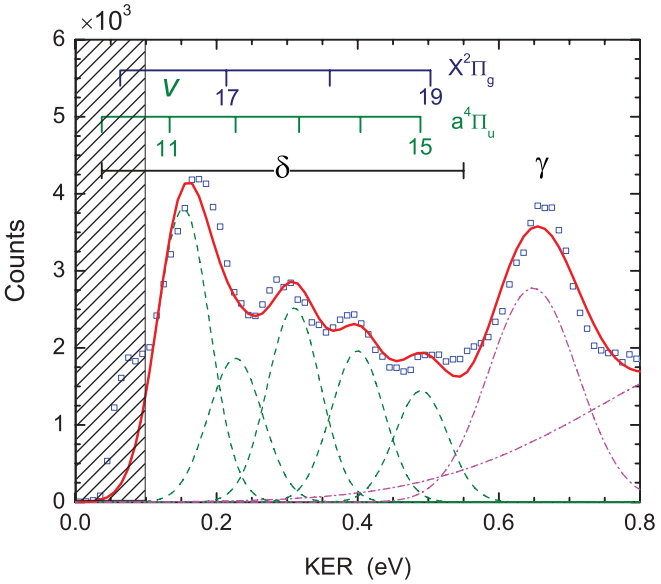

FIG. 3. (Color online) The low-KER spectrum of O_2^+ dissociating into O^++O in a 790-nm, 40-fs, 4×10^{15} W/cm^2 laser pulse. The fit function (thick red line), consisting of the γ (dash-dot magenta line) and δ (dashed green line) contributions (see text), is in good agreement with the data (open blue squares). A tail of the peak centered around 1 eV (see Fig. 2) is also visible at high KER (dash-dot magenta line). Note that the $v = 12$ is suppressed (see text). The blue vertical ticks at the top mark the expected positions for dissociation of the $X\,^2\Pi_g$ state, following the pathways shown in Fig. 1(a) (see text)—note that these KER values do not match the data as well as those associated with the $a\,^4\Pi_u$ state indicated by the green vertical ticks.

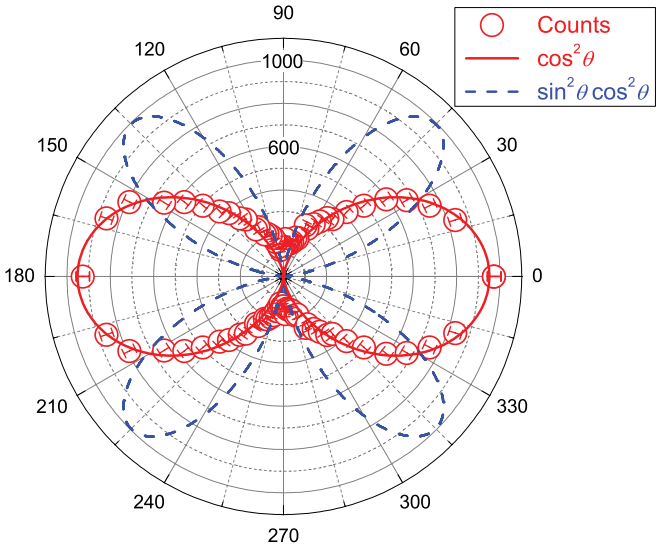

FIG. 4. (Color online) A polar plot of the O^++O dissociation direction relative to the laser polarization (the distribution was reflected about the polarization axis to generate the bottom part of the polar plot). Error bars are smaller than the symbols. The solid red line is a $\cos^2\theta$ distribution that fits the data well, while the dashed blue line indicates a $\sin^2\theta\cos^2\theta$ distribution which does not match the data (see text).

of the O_2^+ $a\,^4\Pi_u$ state to the $^4\Sigma_u^+$ state dressed by three photons, although the exact pathway connecting these states requires further discussion [37].

While these features are interesting in their own right, the focus of the present work is on the series of closely spaced, narrow, low-KER peaks labeled δ that have not been observed or discussed before. For visualization, we zoom in on the KER spectrum below 0.8 eV as shown in Fig. 3. Based on their energy we suggest that all the KER peaks labeled δ are due to dissociation of the $v = 11$–15 states bound in the $a\,^4\Pi_u$ potential, along the pathway $|a\,^4\Pi_u\rangle \rightarrow |f\,^4\Pi_g - 1\omega\rangle$ [see Fig. 1(b)]. This is a net one-photon bond softening process similar to the one commonly observed in H_2^+ [38,39]. Specifically, the peaks are centered about the energies one would expect for dissociation by absorption of a 790 nm photon, marked by vertical ticks on Fig. 3.

The data in Fig. 3 is in good agreement with a fit function consisting of the sum of Gaussian peaks centered at the expected positions for $a\,^4\Pi_u(v)$ ($v = 11$–15) to $f\,^4\Pi_g$ transitions, and a couple of additional peaks at higher KER (specifically the γ peak and one additional Gaussian to represent the tail extending to lower KER from the peak(s) centered around 1.0 eV in Fig. 2). A common width was used for the first 5 δ peaks as expected for similar transitions [3], while the width of the remaining 2 peaks were free parameters. Note that the lowest expected KER peak ($v = 10$) cannot be measured in our setup due to losses of very low KER fragments in the Faraday cup, and for the same reason the centroid of the $v = 11$ peak is slightly shifted to a higher energy (the magnitude of this shift is consistent with the one expected when convoluting the response function due to Faraday cup losses with the $v = 11$ Gaussian). Additionally, the dissociation of the $v = 12$ state appears to be suppressed relative to the other states (see discussion below).

To verify the pathway assigned above we present in Fig. 4 the angular distribution associated with events within the δ peaks. The measured angular distribution (open circles) conforms well to a $\cos^2\theta$ distribution as expected for a one-photon $\Pi \rightarrow \Pi$ ($\Delta\Lambda = 0$) transition (see Refs. [30,36]). Moreover, all the peaks in the low-KER feature δ have approximately the same intensity dependence and angular distribution as would be expected for net one-photon transitions between the same electronic states.

While so far we have discussed only dissociation pathways involving the metastable $a\,^4\Pi_u$ state of O_2^+, we can exclude the $X\,^2\Pi_g$ ground state from being responsible for the structure δ for several reasons. First, we identify the most probable dissociation pathways originating from the $X\,^2\Pi_g$ state, shown in Fig. 1(a), as

(i) $|X\,^2\Pi_g\rangle \rightarrow |A\,^2\Pi_u - 1\omega\rangle \rightarrow |^2\Sigma_g^+ - 2\omega\rangle$ and

(ii) $|X\,^2\Pi_g\rangle \rightarrow |^2\Sigma_u^+ - 1\omega\rangle \rightarrow |^2\Sigma_g^+ - 2\omega\rangle$,

following the procedures described in Ref. [30]. Both these pathways involve consecutive one-photon transitions and would yield the same KER since they connect the same initial and final states. In principle, the resulting KER distribution would exhibit vibrational structure over a similar energy range to the δ peaks. However, as can be seen from Fig. 3, the predicted peak positions for the dissociation of the $a\,^4\Pi_u$ state match the data considerably better than those of the $X\,^2\Pi_g$ state. Furthermore, as evident in Fig. 1(a) the Franck-Condon population of the $X\,^2\Pi_g$ v states involved ($v = 16$–19) is

almost negligible as the population is strongly peaked near the bottom of the well. Second, the suggested dissociation pathways of the $X\,^2\Pi_g$ state should have a $\sin^2\theta\cos^2\theta$ angular distribution, as they involve one parallel ($\Delta\Lambda = 0$) and one perpendicular ($\Delta\Lambda = 1$) transition [30], but such a distribution is inconsistent with the measured data, shown in Fig. 4. Finally, the fact that the measured low-KER feature δ persists to relatively low laser intensities (we observe it down to 4×10^{13} W/cm^2, the lowest we have measured) also supports its assignment as a one-photon transition, unlike the net two-photon transition involving the $X\,^2\Pi_g$ state, which we would expect to drop faster with intensity [30].

With this insight at 790 nm, we are able to predict the outcome of dissociation driven by intense 395-nm laser pulses. At 395 nm one expects that all the bound low-v states of $a\,^4\Pi_u$ should decay by $|a\,^4\Pi_u\rangle \rightarrow |f\,^4\Pi_g - 1\omega\rangle$ as the crossing between $a\,^4\Pi_u$ and the dressed $|f\,^4\Pi_g - 1\omega\rangle$ state is near the minimum of the $a\,^4\Pi_u$ potential as shown in Fig. 5(a). The predicted positions of the KER peaks are indicated by the vertical ticks in Fig. 5(c). Indeed they show very good agreement with the measured KER spectrum in Figs. 5(b) and 5(c). This is further illustrated by the nice fit of the sum of Gaussian peaks with a common width centered at the expected positions or, as shown in Fig. 5(c), allowing only for a small (11 meV) common shift to compensate mainly for experimental uncertainties. The fit function also includes a couple of Gaussian peaks (due to other dissociation pathways) on either side of the δ feature as their tails overlap somewhat with this feature. Additionally, the angular distributions are similar to those for 790 nm confirming the proposed net one-photon dissociation pathway.

Careful inspection of Fig. 5(c) reveals an apparent suppression in the dissociation of particular v states, namely $v = 3$ and 5, relative to their neighbors, given that the initial vibrational population in the $a\,^4\Pi_u$ state is smooth as seen in Fig. 1(b). We believe that the $|a\,^4\Pi_u(v_i)\rangle \rightarrow |f\,^4\Pi_g - 1\omega\rangle$ transitions for $v = 3$ and 5 are suppressed due to the small magnitude of the dipole transition moments coupling these states at this photon energy (Cooper dissociation minima)—a phenomena we have recently observed in H_2^+ dissociation [24]. The same holds for the suppressed dissociation of $v = 12$ at 790 nm shown in Fig. 3. Further experimental and theoretical work is ongoing to investigate this vibrational suppression phenomenon in more detail.

B. O_2 target

We have observed similar structure in the dissociative ionization of an O_2 gas target, using VMI as an imaging technique. The specific setup is described elsewhere [40]. In brief, the 790-nm, 8-fs laser pulses passed through the VMI spectrometer and were focused back onto a supersonic jet of O_2 molecules to an intensity of 10^{14} W/cm^2. The resulting O^+ fragments were projected by the ion optics of the VMI spectrometer onto a microchannel plate (MCP) and phosphor assembly. Here we preselected the O^+ ions by gating the MCP bias around the O^+ TOF peak using a triggered high-voltage delay switch.

From the 3D momentum image, we evaluated the KER distribution for dissociation events contained within $\pm 15^\circ$ along $\theta = 90^\circ$, which is shown in Fig. 6. The low-KER spectrum shown in this figure exhibits similar energy structure as observed for the dissociation of the O_2^+ beam target. Furthermore, we can identify the main features as the dissociation of $a\,^4\Pi_u$ $v = 10$–14 states via the pathway $|a\,^4\Pi_u\rangle \rightarrow |f\,^4\Pi_g - 1\omega\rangle$ (see ticks), following the initial ionization of O_2 ($X\,^3\Sigma_g^-$) to O_2^+ ($a\,^4\Pi_u$). Explicitly, the $v = 11$ state appears as a prominent peak around 0.13 eV, while the $v = 10$ state appears around 0.04 eV, partly "masked" by the VMI conversion artifact near zero-KER. Assuming that the $v = 12$ state is suppressed as discussed above for the O_2^+ beam target, the smaller peaks around 0.25 and 0.38 eV can be associated with the $v = 13$–14 states, respectively. These peaks seem to be somewhat shifted to lower KER from their expected field-free position. Such energy shifts are expected in the presence of a strong laser field (see, e.g., Ref. [20]). Moreover, the shift is expected to be larger

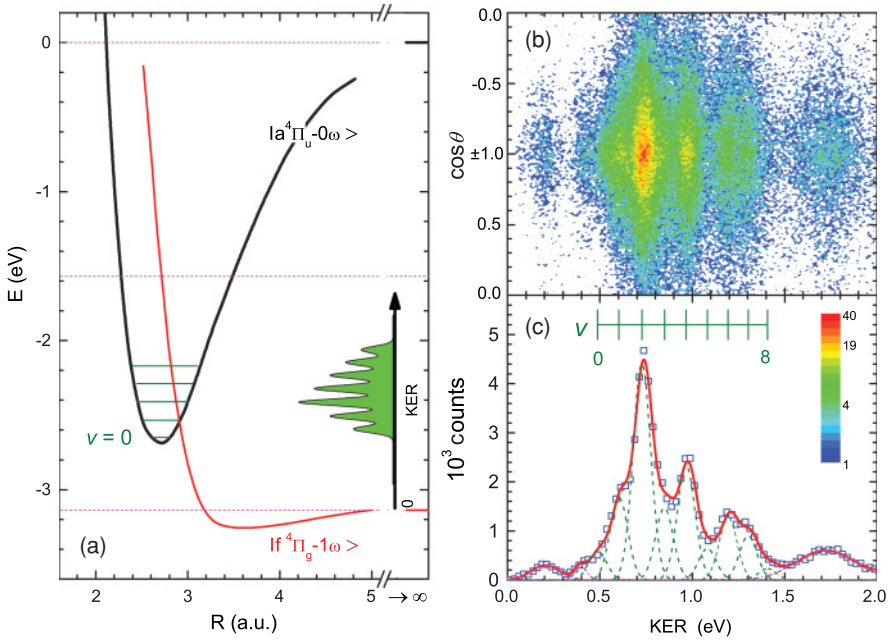

FIG. 5. (Color online) (a) Diabatic dressed potential energy curve diagram of O_2^+ depicting the $|a\,^4\Pi_u\rangle \rightarrow |f\,^4\Pi_g - 1\omega\rangle$ dissociation pathway in a 395-nm laser field. A schematic vibrationally resolved KER spectrum is also shown in the panel. (b) KER-cosθ density plot of O_2^+ dissociation in a 395-nm, 40 fs, 1×10^{14} W/cm^2 laser pulse. (c) The KER spectrum evaluated by integrating over all angles in (b). The measured peaks are in agreement with the position expected for $|a\,^4\Pi_u\rangle \rightarrow |f\,^4\Pi_g - 1\omega\rangle$ transitions from the $v = 0$–8—marked by the vertical ticks. The nice fit to the data (thick red line) consists of Gaussian peaks representing the above transitions (dashed green line) and a couple of free Gaussian peaks on either side of the δ feature (see text). Note that a couple of peaks ($v = 3$ and 5) are suppressed in the spectrum (see text).

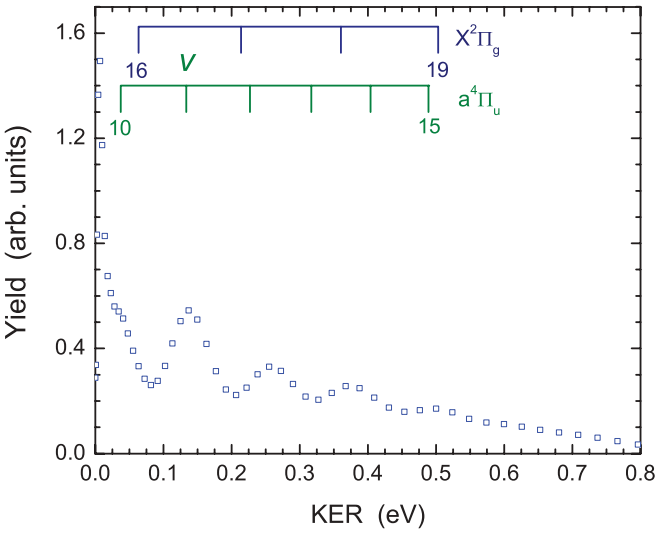

FIG. 6. (Color online) The KER distribution derived after integration of θ over a $\pm 15^\circ$ range around the plane perpendicular to the laser polarization (see text). Note that the spike at about 0.01 eV is most likely an artifact of the conversion from the measured 2D VMI image to 3D [40–42].

in this case because the transient O_2^+ is "born" in a field that is typically stronger than the fields initiating the dissociation of the O_2^+ beam target, where dissociation occurs at the leading edge of the pulse (see, e.g., Refs. [3,43]). Note that the peaks are a worse match to the expected positions for dissociative ionization through the intermediate $X\,^2\Pi_g$ state; however, we cannot rule out some contributions from this state. Pump-probe measurements of this process reveal the relative importance of dissociative ionization via the $a\,^4\Pi_u$ and $X\,^2\Pi_g$ states by analyzing the beat frequency of the vibrational wave packet (see, e.g., Refs. [44,45]) and will be reported elsewhere [42]. The similarities of this KER structure to the one observed for the O_2^+ beam target are remarkable given the difference between the two targets, both in the ionization mechanism forming the dissociating O_2^+ and the nature of their vibrational population—coherent for the O_2 gas target and incoherent for the O_2^+ beam target.

IV. SUMMARY AND OUTLOOK

In summary, vibrationally resolved KER dissociation spectra of a multielectron molecule, O_2^+, by intense ultrashort laser pulses have been measured. The vibrational structure observed persists over a wide range of laser intensities and is present starting from both an O_2 gas target and an O_2^+ ion beam target. We have identified the structure as arising from the dissociation of a subset of vibrational states ($v = 10$–15) of the metastable $a\,^4\Pi_u$ state via the pathway $|a\,^4\Pi_u\rangle \rightarrow |f\,^4\Pi_g - 1\omega\rangle$. In effect this structure is equivalent to that observed previously for bond softening dissociation of H_2^+, although it can be considered as somewhat of a surprise that it survives for a multielectron system considering the complexity of the potential energy curves of O_2^+ (see, e.g., Ref. [30]).

With the ability to perform vibrationally resolved studies one is in a better position to carry out strong-field control experiments targeting specific vibrational states and ultimately leading to a higher level of control. For example, one can envision a pump-probe study of the dissociative ionization of O_2. Since dissociation of individual v states of this molecule can be imaged, as shown here, O_2 would seem a natural candidate to perform such studies, looking, for example, at the effects of the pump pulse on vibrational population [46] or imaging the beat vibrational period from the superposition of neighboring v states [44,45].

ACKNOWLEDGMENTS

We wish to acknowledge the invaluable insight into the underlying process dynamics provided by B. D. Esry over the course of many discussions. We also thank Z. Chang and his group members and C. W. Fehrenbach for assistance with the laser and ion beams, respectively. Supported by the Chemical Sciences, Geosciences, and Biosciences Division, Office of Basic Energy Sciences, Office of Science, U.S. Department of Energy.

[1] M. F. Kling *et al.*, Science **312**, 246 (2006).
[2] G. Sansone *et al.*, Nature **465**, 763 (2010).
[3] B. D. Esry, A. M. Sayler, P. Q. Wang, K. D. Carnes, and I. Ben-Itzhak, Phys. Rev. Lett. **97**, 013003 (2006).
[4] Th. Ergler, A. Rudenko, B. Feuerstein, K. Zrost, C. D. Schröter, R. Moshammer, and J. Ullrich, Phys. Rev. Lett. **97**, 193001 (2006).
[5] A. Staudte *et al.*, Phys. Rev. Lett. **98**, 073003 (2007).
[6] D. Ray *et al.*, Phys. Rev. Lett. **100**, 143002 (2008).
[7] D. Ray *et al.*, Phys. Rev. Lett. **103**, 223201 (2009).
[8] J. McKenna, A. M. Sayler, B. Gaire, N. G. Johnson, K. D. Carnes, B. D. Esry, and I. Ben-Itzhak, Phys. Rev. Lett. **103**, 103004 (2009).
[9] V. Roudnev and B. D. Esry, Phys. Rev. A **76**, 023403 (2007).
[10] R. Dörner, V. Mergel, O. Jagutzki, L. Spielberger, J. Ullrich, R. Moshammer, and H. Schmidt-Böcking, Phys. Rep. **330**, 95 (2000).
[11] J. Ullrich, R. Moshammer, A. Dorn, R. Dörner, L. Ph. H. Schmidt, and H. Schmidt-Böcking, Rep. Prog. Phys. **66**, 1463 (2003).
[12] A. T. J. B. Eppink and D. H. Parker, Rev. Sci. Instrum. **68**, 3477 (1997).
[13] L. Dinu, A. T. J. B. Eppink, F. Rosca-Pruna, H. L. Offerhaus, W. J. van der Zande, and M. J. J. Vrakking, Rev. Sci. Instrum. **73**, 4206 (2002).
[14] J. McKenna *et al.*, Phys. Rev. Lett. **100**, 133001 (2008).
[15] T. T. Nguyen-Dang, H. Abou-Rachid, N. A. Nguyen, N. Mireault, J. Lévesque, K. Vijayalakshmi, and S. L. Chin, Phys. Rev. A **67**, 013405 (2003).

[16] B. A. Khan, S. Saha, and S. S. Bhattacharyya, Phys. Rev. A **73**, 023423 (2006).
[17] A. Giusti-Suzor, F. H. Mies, L. F. DiMauro, E. Charron, and B. Yang, J. Phys. B **28**, 309 (1995), and references therein.
[18] J. H. Posthumus, Rep. Prog. Phys. **67**, 623 (2004), and references therein.
[19] A. Zavriyev, P. H. Bucksbaum, J. Squier, and F. Saline, Phys. Rev. Lett. **70**, 1077 (1993).
[20] K. Sändig, H. Figger, and T. W. Hänsch, Phys. Rev. Lett. **85**, 4876 (2000).
[21] D. Pavičić, T. W. Hänsch, and H. Figger, Phys. Rev. A **72**, 053413 (2005).
[22] P. Q. Wang, A. M. Sayler, K. D. Carnes, J. F. Xia, M. A. Smith, B. D. Esry, and I. Ben-Itzhak, Phys. Rev. A **74**, 043411 (2006).
[23] A. Kiess, D. Pavičić, T. W. Hänsch, and H. Figge, Phys. Rev. A **77**, 053401 (2008).
[24] J. McKenna, F. Anis, B. Gaire, N. G. Johnson, M. Zohrabi, K. D. Carnes, B. D. Esry, and I. Ben-Itzhak, Phys. Rev. Lett. **103**, 103006 (2009).
[25] J. McKenna, A. M. Sayler, B. Gaire, N. G. Johnson, M. Zohrabi, K. D. Carnes, B. D. Esry, and I. Ben-Itzhak, J. Phys. B **42**, 121003 (2009).
[26] V. S. Prabhudesai *et al.*, Phys. Rev. A **81**, 023401 (2010).
[27] This is in contrast to the abundance of vibrationally resolved spectra in beam fragment photodissociation studies (see, for example, Refs. [47-49]). However, the nature of dissociation under the influence of a weak or strong field differs, the first being a single-photon process while the latter is strongly affected by multiphoton phenomena [17,18].
[28] I. Ben-Itzhak, P. Q. Wang, J. F. Xia, A. M. Sayler, M. A. Smith, K. D. Carnes, and B. D. Esry, Phys. Rev. Lett. **95**, 073002 (2005).
[29] I. Ben-Itzhak, in *Progress in Ultrafast Intense Laser Science IV*, Springer Series in Chemical Physics, edited by K. Yamanouchi, A. Becker, R. Li, and S. L. Chin (Springer, New York, 2009), Vol. 91, p. 67
[30] A. M. Sayler, P. Q. Wang, K. D. Carnes, B. D. Esry, and I. Ben-Itzhak, Phys. Rev. A **75**, 063420 (2007).
[31] A. M. Sayler, Ph.D. thesis, Kansas State University, 2008.
[32] A. Tabché-Fouhaillé, J. Durup, J. T. Moseley, J. B. Ozenne, C. Pernot, and M. Tadjeddine, Chem. Phys. **17**, 81 (1976).
[33] B. R. Turner, J. A. Rutherford, and D. M. J. Compton, J. Chem. Phys. **48**, 1602 (1968).
[34] C. M. Marian, R. Marian, and S. D. Peyerimhoff, Mol. Phys. **46**, 779 (1982).
[35] E. Y. Sidky and I. Ben-Itzhak, Phys. Rev. A **60**, 3586 (1999).
[36] A. Hishikawa, S. Liu, A. Iwasaki, and K. Yamanouchi, J. Chem. Phys. **114**, 9856 (2001).
[37] A few dissociation pathways that are consistent with the KER peak labeled γ in Figs. 2 and 3 have been proposed: (i) $|a^4\Pi_u\rangle \rightarrow |2^4\Pi_g^+ - 3\omega\rangle$, (ii) $|a^4\Pi_u\rangle \rightarrow |f^4\Pi_g^+ - 1\omega\rangle \rightarrow |2^4\Pi_g^+ - 3\omega\rangle$ [30], (iii) $|a^4\Pi_u\rangle \rightarrow |f^4\Pi_g^+ - 1\omega\rangle \rightarrow |2^4\Pi_u^+ - 2\omega\rangle \rightarrow |2^4\Pi_g^+ - 3\omega\rangle$ [36].
[38] P. H. Bucksbaum, A. Zavriyev, H. G. Muller, and D. W. Schumacher, Phys. Rev. Lett. **64**, 1883 (1990).
[39] A. Zavriyev, P. H. Bucksbaum, H. G. Muller, and D. W. Schumacher, Phys. Rev. A **42**, 5500 (1990).
[40] S. De, I. Znakovskaya, D. Ray, F. Anis, N. G. Johnson, I. A. Bocharova, M. Magrakvelidze, B. D. Esry, C. L. Cocke, I. V. Litvinyuk, and M. F. Kling, Phys. Rev. Lett. **103**, 153002 (2009).
[41] M. J. J. Vrakking, Rev. Sci. Instrum. **72**, 4084 (2001).
[42] S. De *et al.* (in preparation).
[43] B. D. Esry and I. Ben-Itzhak, Phys. Rev. A **82**, 043409 (2010).
[44] B. Feuerstein, Th. Ergler, A. Rudenko, K. Zrost, C. D. Schröter, R. Moshammer, J. Ullrich, T. Niederhausen, and U. Thumm, Phys. Rev. Lett. **99**, 153002 (2007).
[45] S. De, I. A. Bocharova, M. Magrakvelidze, D. Ray, W. Cao, B. Bergues, U. Thumm, M. F. Kling, I. V. Litvinyuk, and C. L. Cocke, Phys. Rev. A **82**, 013408 (2010).
[46] X. Urbain, B. Fabre, V. M. Andrianarijaona, J. Jureta, J. H. Posthumus, A. Saenz, E. Baldit, and C. Cornaggia, Phys. Rev. Lett. **92**, 163004 (2004).
[47] J. T. Moselev, M. Tadjeddine, J. Durup, J. B. Ozenne, C. Pernot, and A. Tabché-Fouhaillé, Phys. Rev. Lett. **37**, 891 (1976).
[48] H. Helm, P. C. Cosby, and D. L. Huestis, J. Chem. Phys. **73**, 2629 (1980).
[49] J. Moseley and J. Durup, Annu. Rev. Phys. Chem. **32**, 53 (1981), and references therein.